APPENDIX A
KINEMATIC BICYCLE MODEL

The kinematic model of lateral vehicle motion, as described by Rajamani (2006), was used to generate a simulation to identify and evaluate the controller parameters, in terms of the trajectory that is generated. The following set of equations serve as a short overview based on Rajamani's work; as a kinematic model, no interaction forces between vehicle and environment were modeled. The aim of this model is to investigate the effect guidance torques on the steering wheel, applied by the controller, have on the vehicle trajectory.

The kinematic model described serves as a basis for the bicycle model; therefore, both front wheels of the vehicle are described by a single point A, with front wheel angle δ_f, and similarly, both rear wheels are set at point B, with rear wheel angle δ_r. Both are at distance l_f and l_r from vehicle center of gravity C, respectively. The assumption was made that velocity vectors at A and B are in line with the corresponding wheel angle; as such, slip angles were set to zero. Velocity V of point C was set constant, and makes side slip angle β with the vehicle centerline, which can be calculated using equation 34.

$$\beta = tan^{-1}\Big(\frac{l_f tan(\delta_r) + l_r tan(\delta_f)}{l_f + l_r}\Big) \tag{34}$$

Three vehicle state parameters are required; horizontal coordinate X, vertical coordinate Y, and vehicle orientation angle ψ. The rate of change of ψ, referred to as yaw rate $\dot{\psi}$, can be determined using the following formula:

$$\dot{\psi} = \frac{V cos(\beta)}{l_f + l_r} \cdot (tan(\delta_f) - tan(\delta_r)) \tag{35}$$

Assuming rear wheel angle δ_r to be equal to zero, and both l_f and l_r at equal length $\frac{1}{2}l_v$ (wheelbase), equations 34 and 35 are reduced to equations 36 and 37, respectively:

$$\beta = arctan\big(\frac{1}{2} \cdot tan(\delta_f)\big) \tag{36}$$

$$\dot{\psi} = \frac{V cos(\beta)}{l_v} \cdot tan(\delta_f) \tag{37}$$

Moreover, horizontal velocity $\dot{X}$ and vertical velocity $\dot{Y}$ are given by:

$$\dot{X} = V cos(\beta + \psi) \tag{38}$$

$$\dot{Y} = V sin(\beta + \psi) \tag{39}$$

After each time step t_s, vehicle orientation was updated. Steering torques, either by the driver or the support system, act to turn the steering wheel by δ_{sw} degrees. For this end, the following state space equation was used:

$$\begin{bmatrix} \ddot{\delta}_{sw} \\ \dot{\delta}_{sw} \end{bmatrix} = \begin{bmatrix} -\frac{B_w}{J_w} & -\frac{K_w}{J_w} \\ 1 & 0 \end{bmatrix} \cdot \begin{bmatrix} \dot{\delta}_{sw} \\ \delta_{sw} \end{bmatrix} + \begin{bmatrix} \frac{T_{steering}}{J_w} \\ 0 \end{bmatrix}$$

With $\dot{\delta}_{sw}$ and $\ddot{\delta}_{sw}$ steering wheel angular velocity and angular acceleration, respectively. J_w, B_w and K_w are steering wheel inertia, damping and centering stiffness, and $T_{steering}$ represents the torques presented onto the steering wheel.

Finally, steering wheel angle is translated to front wheel angle, using the steering ratio:

$$\delta_f = \frac{\delta_{sw}}{Steering\,ratio} \tag{40}$$

APPENDIX B
CONTROLLER TUNING

The aim of this research was to design haptic steering guidance to support human drivers, in a manner to reduce the prevalence of conflict torques. To this end, the control structure described in section 2 was developed. In this appendix, the method used for parameter identification will be put forward: (1) vehicle parameters and controller functionality; (2) identification using human data; (3) sensitivity analysis around identified parameter settings; and (4) final settings for shared control.

1) Vehicle parameters and controller functionality: The effect of different control parameters on guidance torques, as function of TLC, is illustrated in figure 10. Note that this is not an actual representation of guidance torques in the driving task; instead, it serves to visualize the response to different parameter settings. In the simulation, the parameters listed in table II were used. They were matched to those used in a simulator study conducted by (De Nijs, 2011). Driver data collected was used for parameter identification, as will be put forward in the next section. As a preliminary analysis, it was investigated whether different trajectories could be generated by the control structure, as visualized in figure 11. The trajectories were generated using full automation; no driver input was modeled. A distinction can be seen between lenient control settings, which strongly cuts the curve, and strict control settings, which steers alongside the center line of the road. The control parameters listen in table III were used. For both driving conditions, the same left curve with inner curve radius 300 m was used. For this road, as well as all subsequent roads discussed in this appendix, road profile started with 51 m. of straight driving, followed by 115 m curve, and another straight section of 51 m. Velocity was kept constant throughout the driving task.

TABLE II: Vehicle parameters used for the simulation

Variable	Value
Simulation update time t_s [s]	0.05
Wheelbase l_v [m]	2.8
Velocity V [$\frac{m}{s}$]	20
Steering ratio [-]	40
Steering wheel inertia J_w [$\frac{Nms^2}{deg}$]	0.2
Steering wheel damping B_w [$\frac{Nms}{deg}$]	2.0
Steering wheel stiffness K_w [$\frac{Nm}{deg}$]	4.2

2) Parameter identification: Controller parameters were identified based on human driver data. Twelve participants repeated three trials each, on 6 different curvature profiles; inner curve radii of 150 m, 200 m and 300 m were presented, both towards the left and towards the right. The mean and standard deviation, for lateral error and steering wheel angle, are visualized in figures 12 and 13, respectively.

A range of initial parameter settings was determined heuristically, and a grid search within this range for the four parameters was conducted. Resultant lateral error and steering angle profile were compared to human data for each of the six curvature conditions, using the Variance Accounted For (equation 33). For identical datasets, VAF returns 100 %. Conversely, VAF values below 0 % indicate negative response; a straight line would have yielded better performance. Parameter settings with highest overall VAF for all six road curvatures, for both lateral error and steering wheel angle, were determined. Parameter range, incremental step size and final values are summarized in table IV. Note that K_{cbg}, the torque gain, was set constant. As no driver torques were modeled, instead investigating controller performance, equal error signal to torque (equation 32) ratio was ensured, for valid comparison between controller settings. The influence of K_{cbg} on steering response and trajectory will be discussed in the sensitivity analysis.

TABLE III: Simulation settings for controller parameters, for both a lenient and a strict setting.

Variable	Value - lenient	Value - strict
Driver uncertainty λ [$\frac{1}{m}$]	0.0001	0.01
Minimum correction ϕ [-]	0.1	0.1
Maximum correction θ [-]	30	10
Weighing ratio γ [-]	10	0.1
Torque gain K_{cbg} [Nm]	5	5

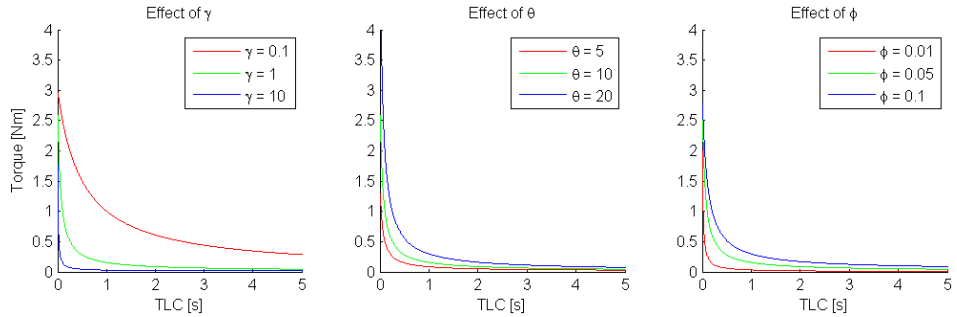

Fig. 10: Effect of weighing ratio γ, maximum correction θ and minimum correction ϕ . Base parameters settings were γ = 1, θ = 10 and ϕ = 0.05.

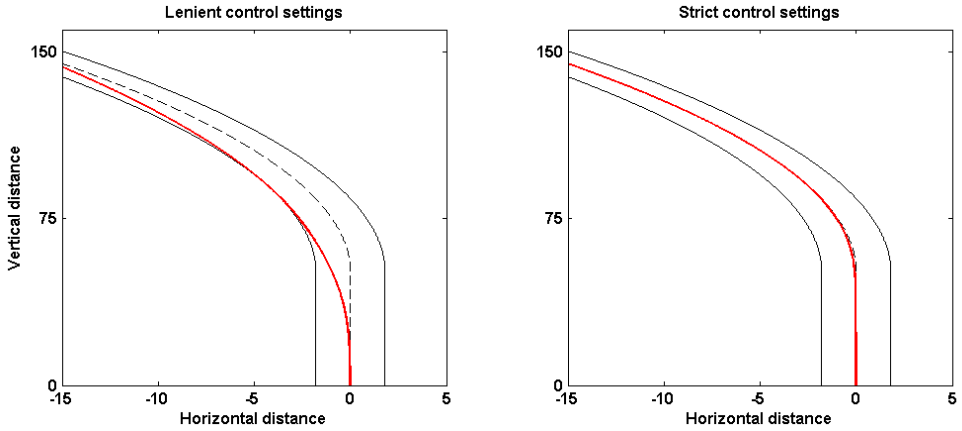

Fig. 11: Vehicle trajectory using two different control settings. Vehicle was driven over a road (width 3.6 m, inner curve radius 300 m) at 20 m/s. On the left, controller settings were lenient, supporting distinct curve cutting behavior by the automation. On the right, controller settings were strict; the vehicle stayed close to the center line. Note that the scale of axes is unequal.

In figure 14, the comparison between human and model lateral error and yaw rate is visualized. For all six conditions, a close match between the two is found for yaw rate, indicating equal steering response over the trajectories. On the other hand, the generated trajectories, and the corresponding lateral error, do not closely match the human trajectory for all conditions; due to the large differences in curve negotiation strategy, rather than the fixed strategy employed by the support system, differences between conditions are large (Saleh et al., 2013). Particularly right curves, in which the driver maintained deviation from the center line throughout the task, were different from controller trajectory. Interestingly, the close match between yaw rate does not serve to predict a match in lateral error; large differences in lateral error can be produced by relatively small differences in yaw rate (Kolekar et al., 2016). Note that the driving task continued before and after the investigated road sections; as such, an offset in lateral is present. The results of the VAF analysis are summarized in table V.

TABLE IV: Parameter values for grid search, indicating minimum and maximum values, as well as incremental step size. Final settings, following VAF analysis, are included.

Variable	Min	Max	Increment	Final
Driver uncertainty λ [$\frac{1}{m}$]	0.001	0.006	0.001	0.006
Minimum correction ϕ [-]	0.05	0.25	0.05	0.05
Maximum correction θ [-]	10	100	10	100
Weighing ratio γ [-]	0.02	0.2	0.02	0.04

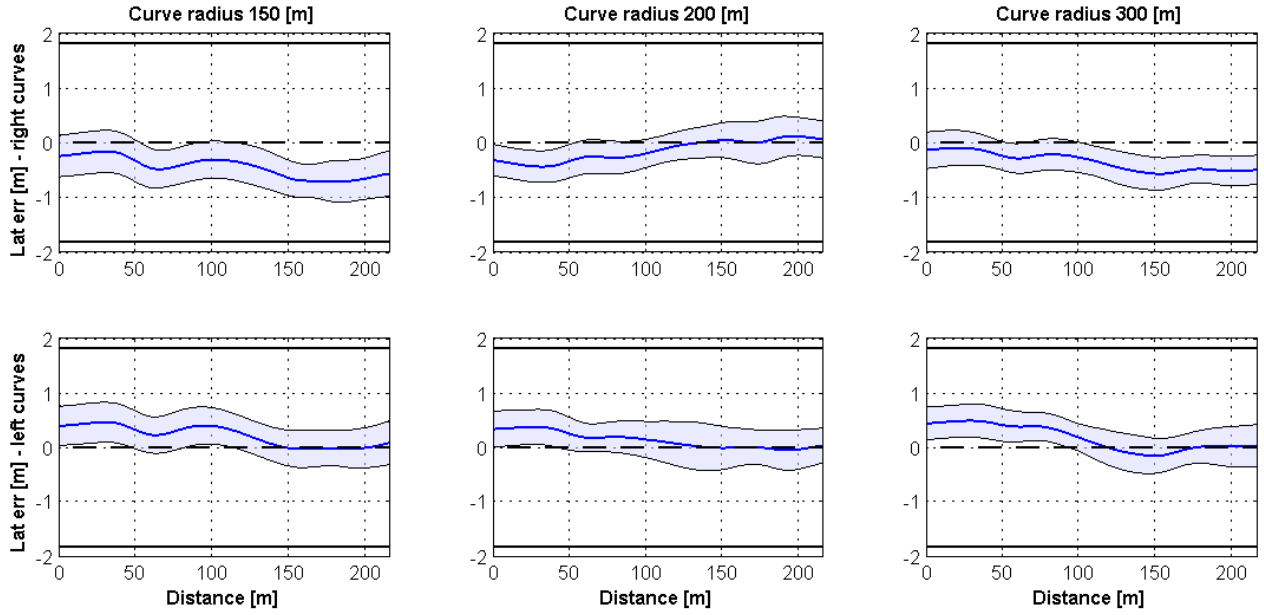

Fig. 12: Driver lateral error as function of distance. Visualized are mean result over all participants (solid blue line) and standard deviation (light blue area), as well as lane centerline and lane boundaries. Right curves (top) and left curves (bottom) were investigated for inner curve radius 150 m (left), 200 m (center) and 300 m (right).

TABLE V: Parameter values for grid search, indicating minimum and maximum values, as well as incremental step size. Final settings, following VAF analysis, are included.

Driving condition	Lat err VAF [%]	SW angle VAF [%]
Left - 150 m	-34.56	97.87
Left - 200 m	-8.52	98.64
Left - 300 m	47.44	97.32
Right - 150 m	-83.11	98.08
Right - 200 m	22.28	98.41
Right - 300 m	-48.84	99.01

3) Sensitivity analysis: In order to investigate the relative influence of parameters in determining trajectory and steering response, a sensitivity analysis was conducted. The identified parameter settings (table IV) were halved or doubled; VAF was subsequently computed to investigate the relative order of effect. Note that the sensitivity analysis was solely conducted on the leftwards curve with inner curve radius 300 m. The reported VAF values therefore serve to illustrate the relative effect of a parameter on vehicle trajectory and steering wheel angle, rather than as absolute influence on controller performance.

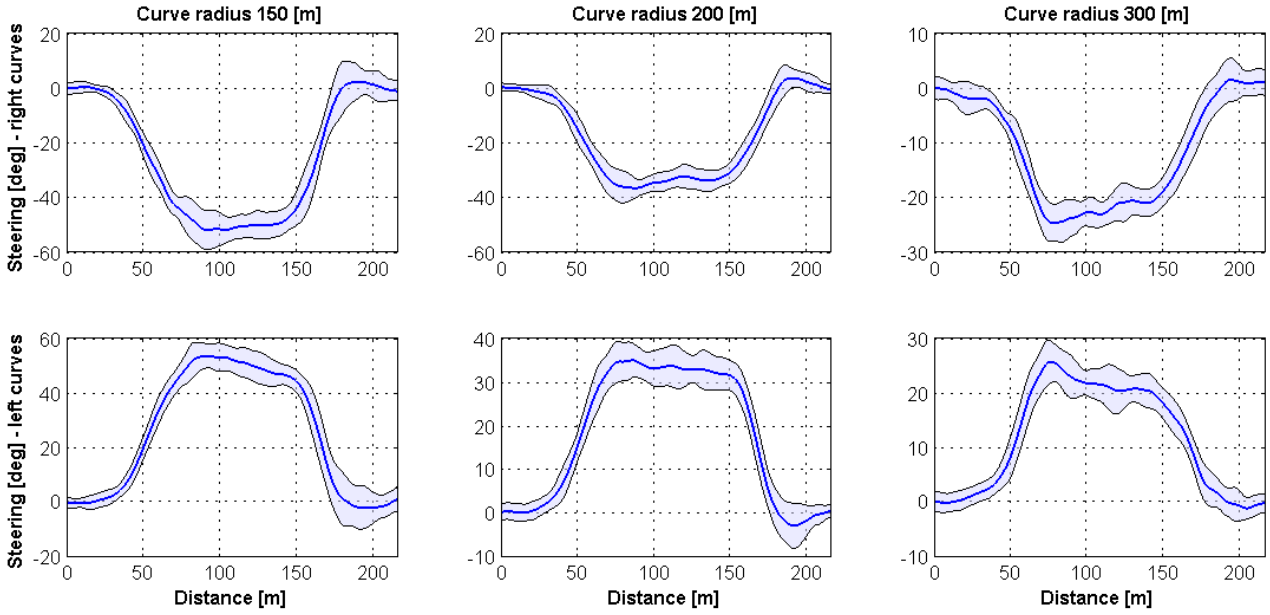

Fig. 13: Driver steering angle as function of distance. Visualized are mean result over all participants (solid blue line) and standard deviation (light blue area). Right curves (top) and left curves (bottom) were investigated for inner curve radius 150 m (left), 200 m (center) and 300 m (right).

TABLE VI: Sensitivity analysis. 50 % and 200 % of parameter settings were investigated, and corresponding VAF values for lateral error (LE) and steering response in terms of yaw rate (SW) were computed.

	Results at 50 %			Results at 200 %		
Variable	**Value**	**LE VAF [%]**	**SW VAF [%]**	**Value**	**LE VAF [%]**	**SW VAF [%]**
λ [$\frac{1}{m}$]	0.003	38.49	96.40	0.012	22.98	95.79
γ [-]	0.02	46.36	97.34	0.08	46.45	97.33
θ [-]	50	37.96	97.38	200	52.14	96.63
ϕ [-]	0.025	46.45	97.33	0.1	46.36	97.34
K_{cbg} [Nm]	2.5	37.97	97.38	10.0	52.14	96.63
K_w [$\frac{Nm}{deg}$]	2.1	50.93	97.31	8.4	38.69	97.34
B_w [$\frac{Nms}{deg}$]	1.0	47.92	96.98	4.0	46.70	97.47
J_w [$\frac{Nms^2}{deg}$]	0.1	-189.12	-913.99	0.4	47.52	97.03

The aim of the sensitivity analysis serves two purposes. First, it allows for the identification of critical parameters that influence the trajectory or steering behavior. Second, it can be used for individualization of controller settings; different individuals require (and desire) different types of control feedback, as argued by (Byrne and Parasuraman, 1996; Wilson et al., 2006). Therefore, four additional parameters were included in the sensitivity analysis: steering wheel rotational inertia J_w, steering wheel rotational damping B_w, steering wheel centering stiffness K_w, and torque gain K_{cbg}. In the analysis, all parameters were kept at base settings, previously described in tables IV and II. Each parameter was halved (50 %) of previously identified setting, and doubled (200 %), for a total of 16 additional parameter settings. Table VI contains parameter settings at 50 % and at 200 %, respectively, and corresponding VAF values for both lateral error and yaw rate, which serves as measure of steering wheel angle. Responses of each parameter, for both lateral error and yaw rate, are visualized in figures 15 and 16, respectively.

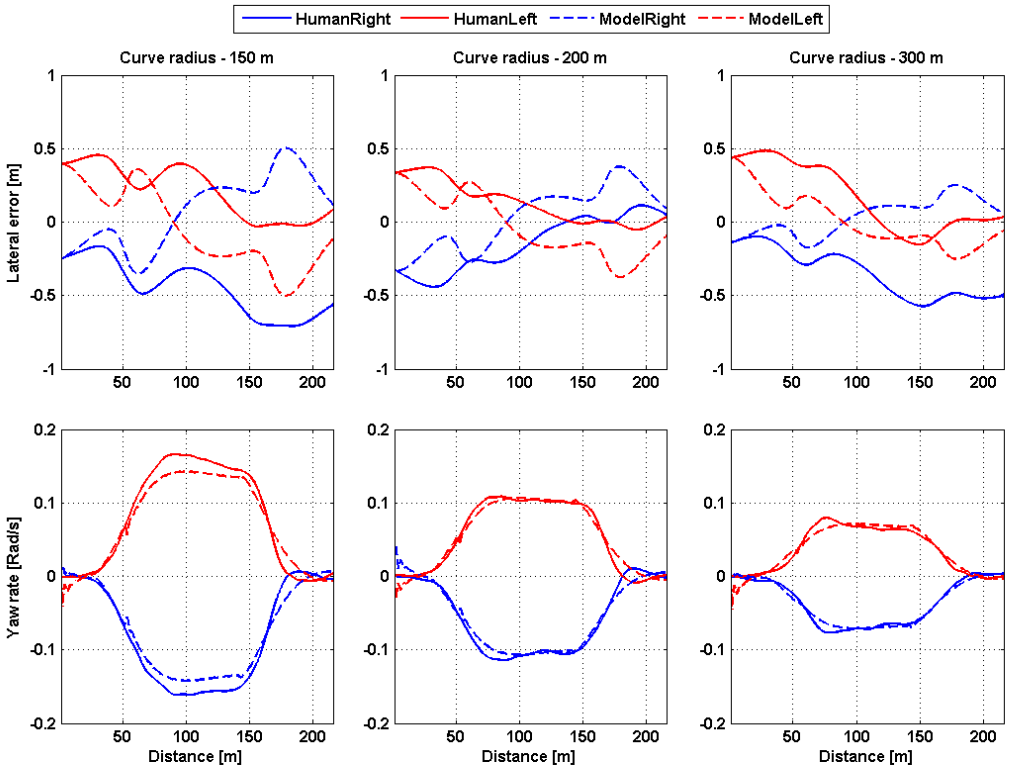

Fig. 14: Trajectory and steering response for six curvature profiles. Positive lateral error is left of the centerline [m]. Positive yaw rate corresponds to steering to the left [rad/s]. Visualized are human (solid line) and model (dashed line) response, on right (blue) and left (red) curves. Inner curve radii of 150 m (left), 200 m (center) and 300 m (right) were presented. Overall, yaw rate comparison produced high VAF, indicating close match between human and automation steering action. VAF results for lateral error varied between conditions.

Worth noting is, foremost, that little difference in response, for either 50 % parameter setting or 200 % parameter setting, was discovered for yaw rate. Indeed, compared to the original steering VAF (97.32 %) the largest increase was reported at 50 % of either maximum correction θ or torque gain K_{cbg}, at 97.38 %. An incredibly large decrease was discovered for steering wheel inertia $J_w = 0.1$, at a VAF of -913.99 %. Visual inspection clearly shows unstable steering behavior; due to the low inertia, controller corrections continually overshoot. Aside for this parameter setting, largest decrease was at uncertainty parameter $\lambda = 0.012$, with a VAF of 95.79. Indeed, visual inspection shows initial oscillations (also visible for θ, K_{cbg} and B_w); the functional boundaries of the controller are thereby in this region for the aforementioned parameters.

Similar to table V, a wide difference in VAF % was reported for lateral error. At base parameter settings, a VAF of 47.44 % was achieved. The largest increase, at 52.14 %, was discovered for both $\theta = 200$ and $K_{cbg} = 10.0$, followed by 50.93 % for $K_w = 2.1$. The largest decrease in VAF was reported for $J_w = 0.1$, which produced unstable control behavior. Following that, largest decrease was reported for $\lambda = 0.012$ (VAF = 22.98 %). From the VAF analysis (table VI, as well as visual inspection of figures 15 and 16, several recommendations can be drawn. First, unstable behavior occurs at decreasing values of J_w, and presumably at parameter settings of $\lambda < 0.003$, $\theta > 200$, $K_{cbg} > 10$ and $B_w < 1.0$. For individualization, most influential parameters are λ, θ, K_{cbg} and K_w, which show the biggest differences in achieved trajectory.

4) Settings for Haptic Steering Guidance: So far, all analyses were conducted at full automation, excluding the influence of any human operator. To ensure cooperation between driver and steering support system, the parameters settings were heuristically tuned in the driving simulator setup. The final control parameters are reiterated in table VII. At these parameter settings, automation was unable to follow the curve. It is therefore required for the human operator to continuously interact with the steering wheel for correct curve negotiation, which is one of the criteria put forward by Abbink et al. (2011).

TABLE VII: Final control parameters.

Variable	Value
λ [$\frac{1}{m}$]	0.004
γ [-]	0.1
θ [-]	10
ϕ [-]	0.01
K_{cbg} [Nm]	0.3
K_w [$\frac{Nm}{deg}$]	4.2
B_w [$\frac{Nms}{deg}$]	2.0
J_w [$\frac{Nms^2}{deg}$]	0.2

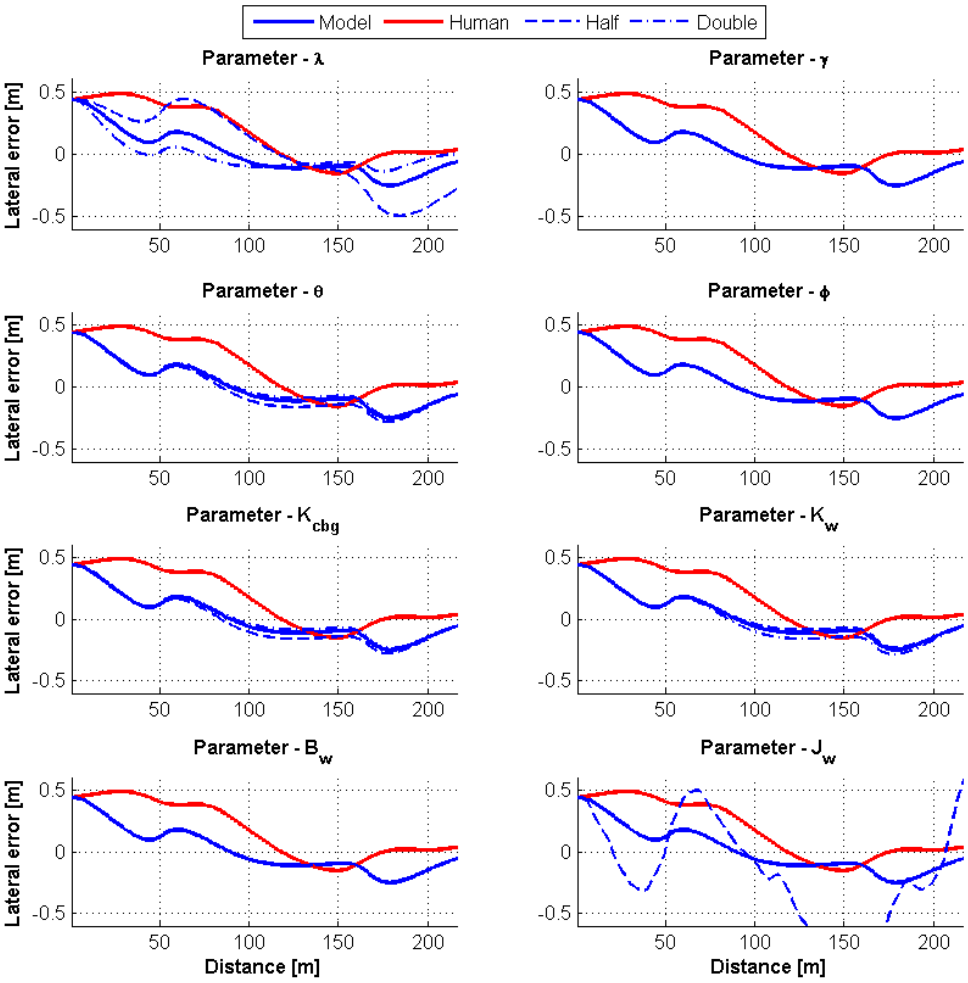

Fig. 15: Sensitivity analysis results for lateral error, on a left curve with inner curve radius 300 m. Lateral error at base settings is visualized as solid blue line, corresponding human driver data as solid red. The effect of each individual parameter at half the base setting (dashed) and double base setting (dash dot) is visualized. Parameter influence was investigated for driver uncertainty λ, weighing ratio γ, maximum yaw rate correction θ, minimum yaw rate correction ϕ, torque gain K_{cbg}, steering wheel centering stiffness K_w, steering wheel rotational damping B_w, and steering wheel rotational inertia J_w.

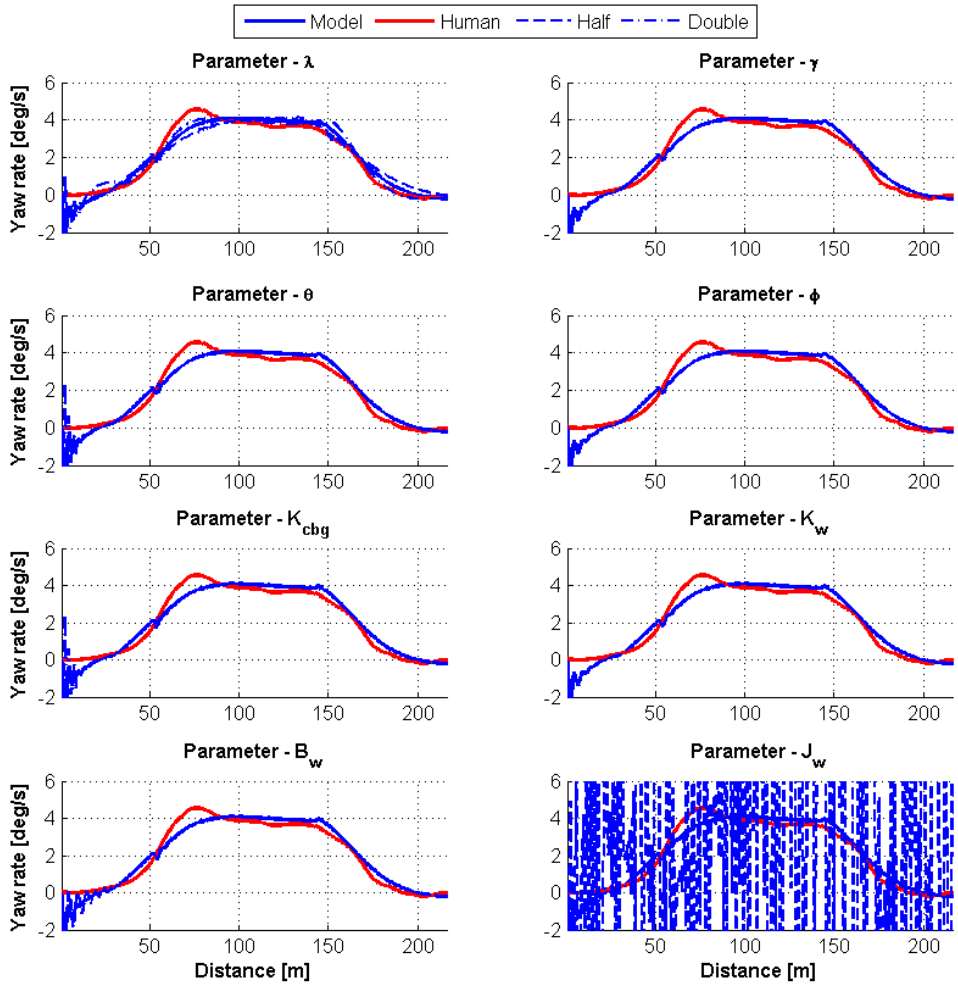

Fig. 16: Sensitivity analysis results for yaw rate, an indicator of steering response, on a left curve with inner curve radius 300 m. Yaw rate at base settings is visualized as solid blue line, corresponding human driver data as solid red. The effect of each individual parameter at half the base setting (dashed) and double base setting (dash dot) is visualized. Parameter influence was investigated for driver uncertainty λ, weighing ratio γ, maximum yaw rate correction θ, minimum yaw rate correction ϕ, torque gain K_{cbg}, steering wheel centering stiffness K_w, steering wheel rotational damping B_w, and steering wheel rotational inertia J_w.

APPENDIX C
ADDITIONAL TABLES

TABLE VIII: Statistical results for pairwise comparison - Bonferroni corrected significance level of α = 0.05.

Variable	1-2	1-3	2-3	4-5	4-6	5-6	1-4	2-5	3-6
Mean absolute lateral error [m]	$<$ 0.0001	$<$ 0.0001	0.0566	$<$ 0.0001	0.0033	0.0009	$<$ 0.0001	$<$ 0.0001	$<$ 0.0001
Peak absolute lateral error [m]	$<$ 0.0001	$<$ 0.0001	0.0520	$<$ 0.0001	0.0001	0.0125	0.0002	$<$ 0.0001	$<$ 0.0001
Median TLC [s]	0.0001	0.0007	0.0073	0.0016	0.0924	0.1191	$<$ 0.0001	$<$ 0.0001	$<$ 0.0001
Minimum TLC [s]	0.0002	0.0009	0.4682	0.2014	0.0173	0.6871	$<$ 0.0001	$<$ 0.0001	$<$ 0.0001
NASA-TLX [%]	0.0001	0.0107	0.0470	0.0616	0.0209	0.9410	0.0004	0.0745	0.0015
SWRR [s^{-1}]	0.0003	0.0503	0.0211	0.0021	0.1820	0.0454	0.0025	0.0211	0.0309
Mean abs driver torque [Nm]	$<$ 0.0001	$<$ 0.0001	$<$ 0.0001	$<$ 0.0001	$<$ 0.0001	0.0202	$<$ 0.0001	0.1015	$<$ 0.0001
Mean abs feedback torque [Nm]	-	-	0.7515	-	-	$<$ 0.0001	-	0.0001	$<$ 0.0001
VDL acceptance [-]	-	-	0.4184	-	-	0.9556	-	0.0526	0.9413
VDL satisfaction [-]	-	-	0.3435	-	-	0.2694	-	0.1191	0.0816

TABLE IX: Results of 2-way repeated measures ANOVA to investigate if left and right curves are significantly different. Independent factors were driving condition (6) and curve direction (2). All p-values are below the threshold of $\alpha = 0.05$, indicating significant difference for all metrics.

Statistical difference between left and right curves	
Variable	**p-value and (F-value)**
Mean absolute lateral error [m]	2.4993e-04 (18.7130)
Peak absolute lateral error [m]	3.3844e-05 (26.3126)
Standard deviation of lateral error [m]	9.9692e-06 (31.6714)
Median TLC [s]	7.6446e-06 (32.9141)
10th percentile TLC [s]	4.7887e-05 (24.8940)
Minimum TLC [s]	1.3994e-04 (20.7788)
SWRR [s^{-1}]	0.0072 (8.6814)
Mean abs driver torque [Nm]	0.0330 (5.1478)
Mean abs feedback torque [Nm]	0.0011 (13.8398)

APPENDIX D
ADDITIONAL FIGURES

Individual components of the NASA-TLX questionnaire (Mental Demand; Physical Demand; Temporal Demand; Performance; Effort; Frustration) are visualized in figure 17. Results of the driver acceptance questionnaire, are plotted against each other for individual participants, as well as overall response, in figure 18. Raw data, as function of distance, is visualized in figures 19 and 20, for the normal and wide roads, respectively. Each line represents an individual participant. Figure 21 and visualize means driving response, averaged over all participants per condition, for normal road width (figure 9 contains mean driving response for the wide road width). Figures 22, 23, 24 and 25 illustrate lateral distribution, TLC distribution, guidance torques as function of TLC and average response over all participants, respectively. Left columns correspond to left curved sections, right columns to right curved sections.

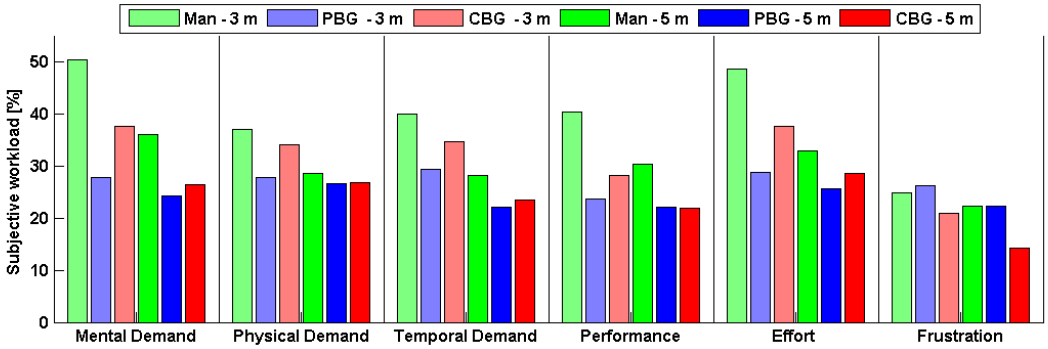

Fig. 17: Scores for the six elements of the NASA-TLX: (1) Mental Demand; (2) Physical Demand; (3) Temporal Demand; (4) Performance; (5) Effort; (6) Frustration. Lower percentage scores correspond to lower subjective workload (i.e. easier to execute task).

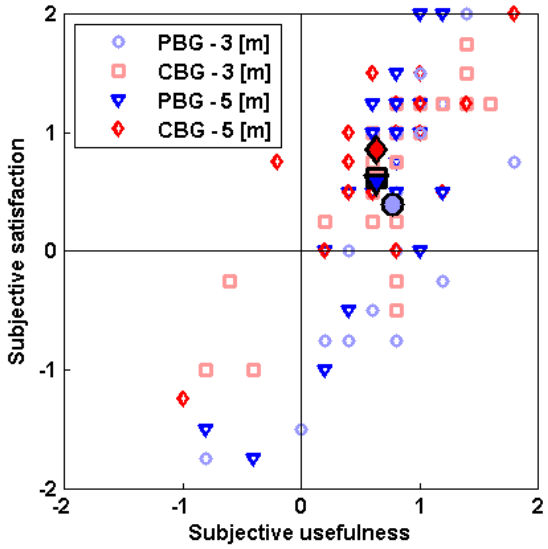

Fig. 18: Subjective usefulness and satisfaction of the Van der Laan questionnaire. Visualized are individual results (small markers) and mean results (large markers), for all four trials for which guidance torques were presented: road width 3 meters, PBG (light blue, circle) and CBG (light red, square), road width 5 meters, PBG (dark blue, triangle) and CBG (dark red, diamond).

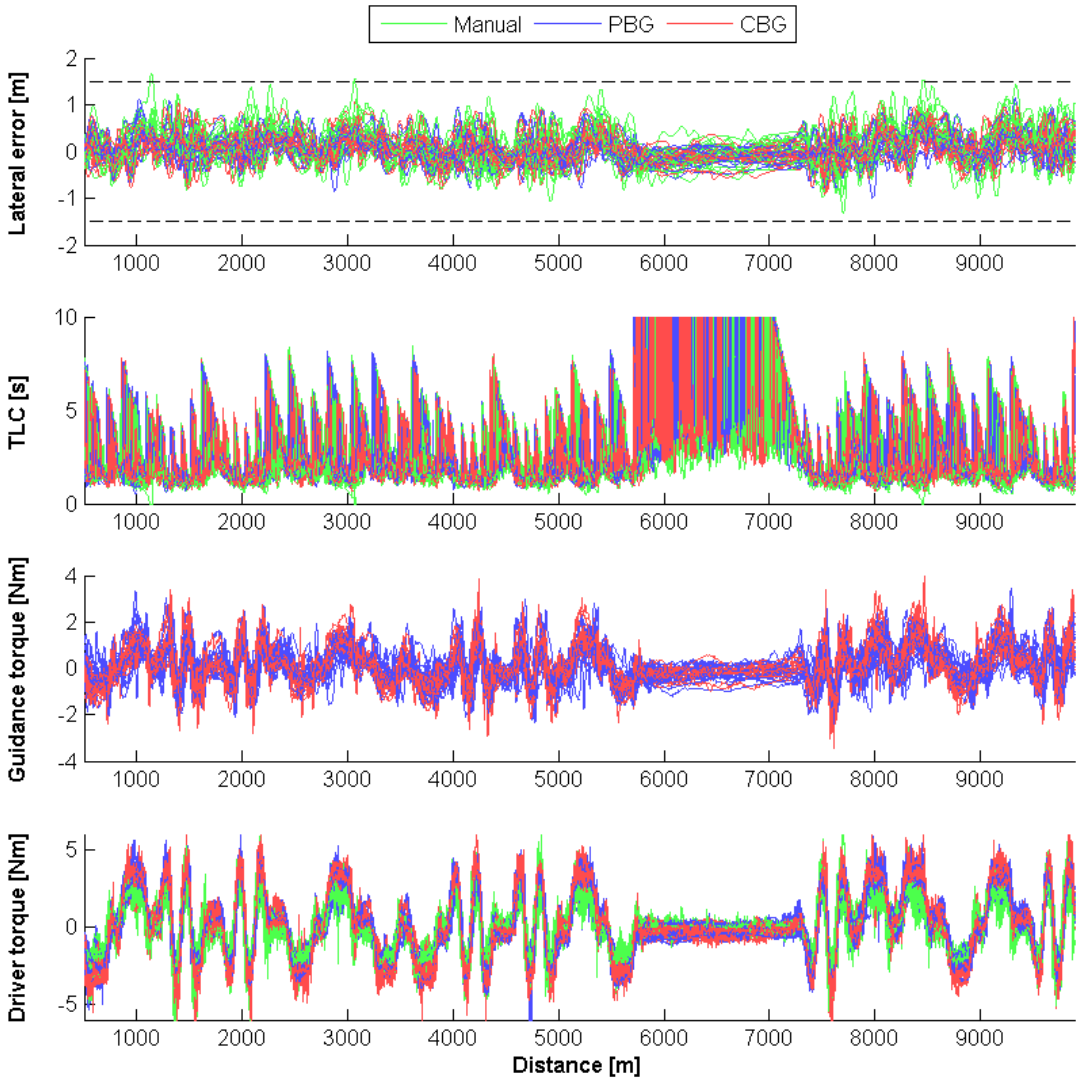

Fig. 19: Individual parameters as function of distance for driving on a normal road (width = 3 m).

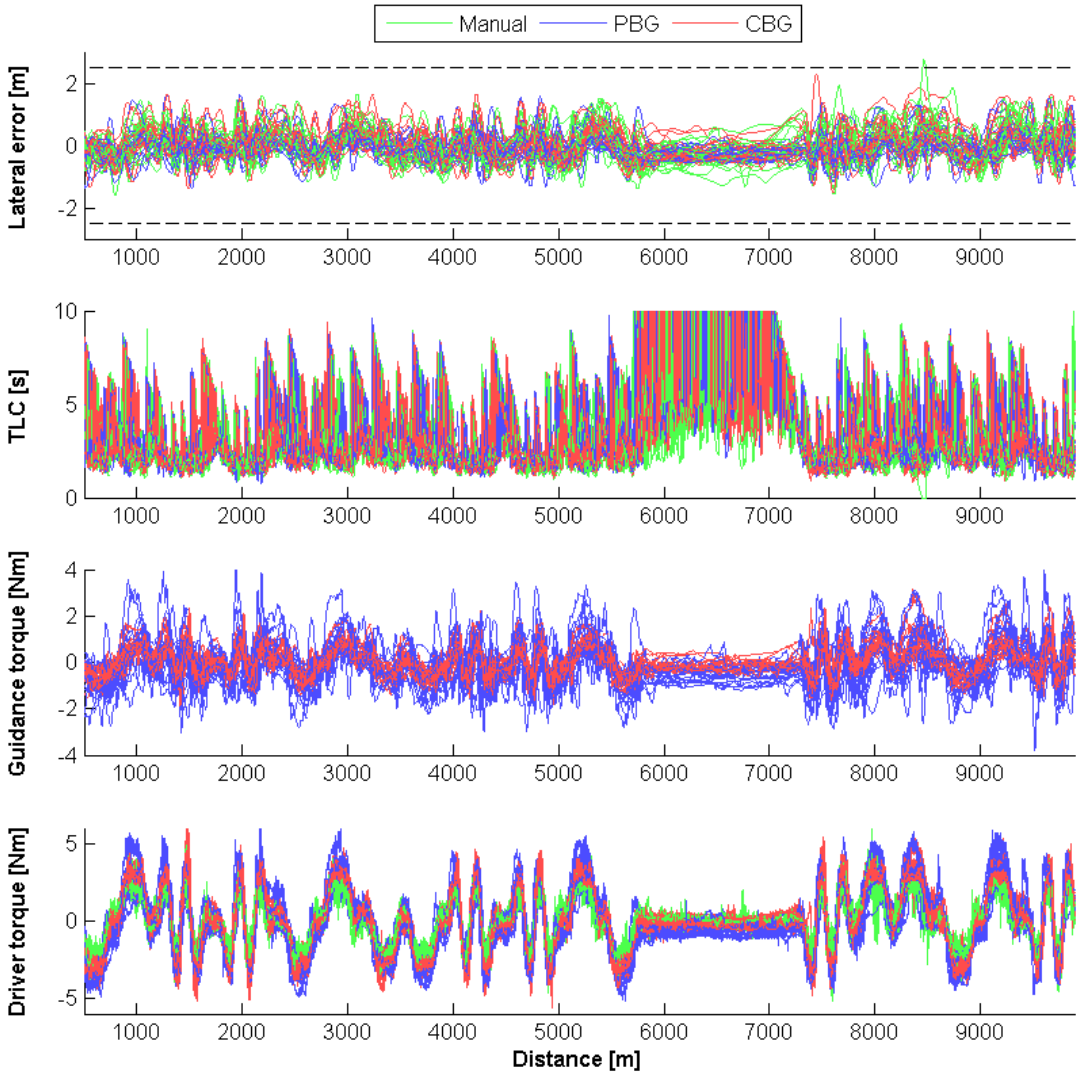

Fig. 20: Individual parameters as function of distance for driving on a wide road (width = 5 m).

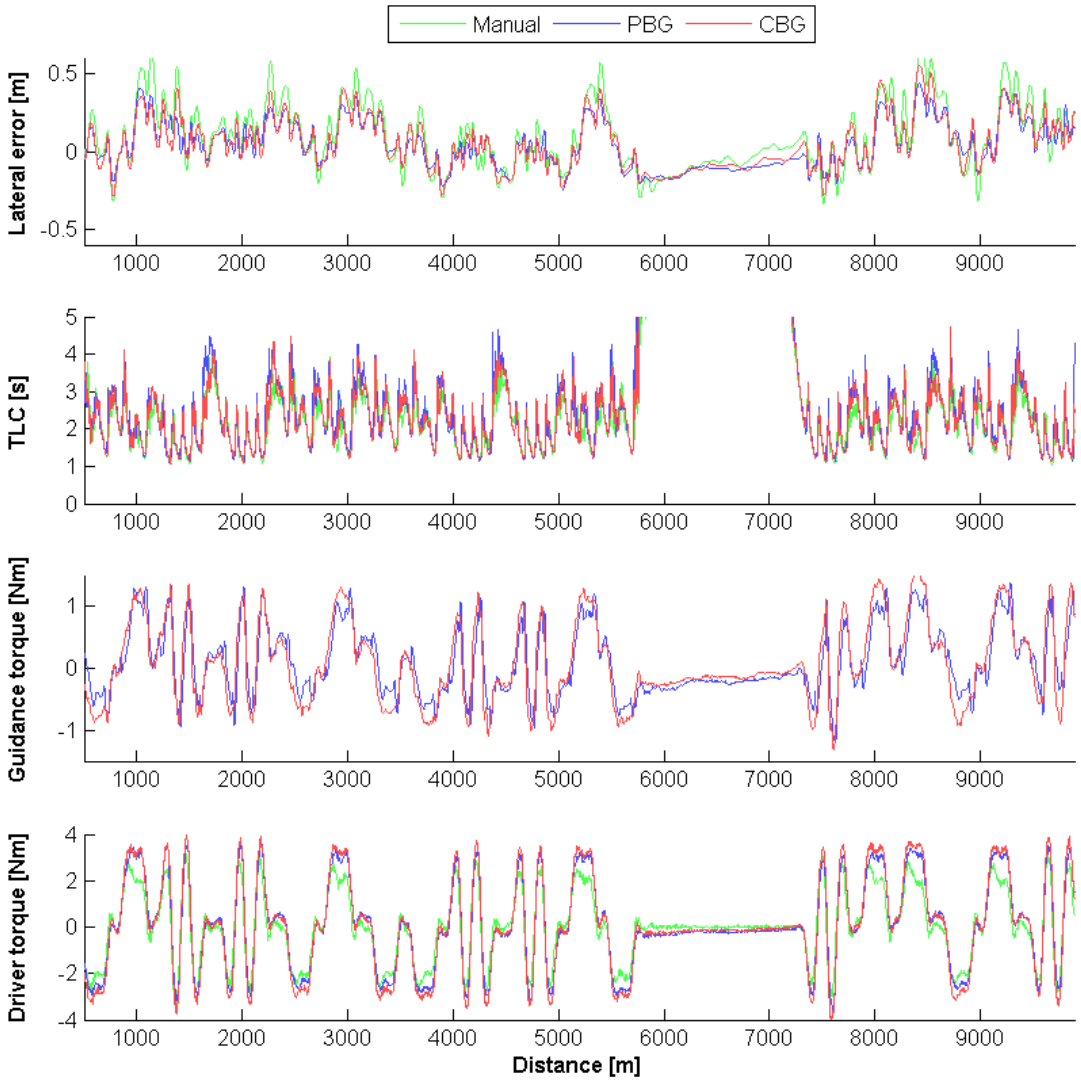

Fig. 21: Mean parameters as function of distance for driving on a normal road (width = 3 m).

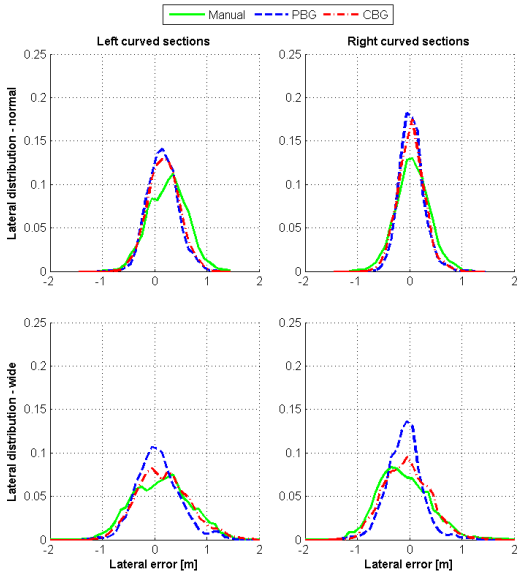

Fig. 22: Distribution of lateral position on the road, averaged over all participants, for road width 3 m (top figures) and road width 5 m (bottom figures), on left curved sections (left figures) and right curved sections (right figures). Depicted are manual driving (green, solid), driving with Performance-Based Guidance (blue, dashed), and driving with Criticality-Based Guidance (red, dash-dot). Bin size was 0.1 m.

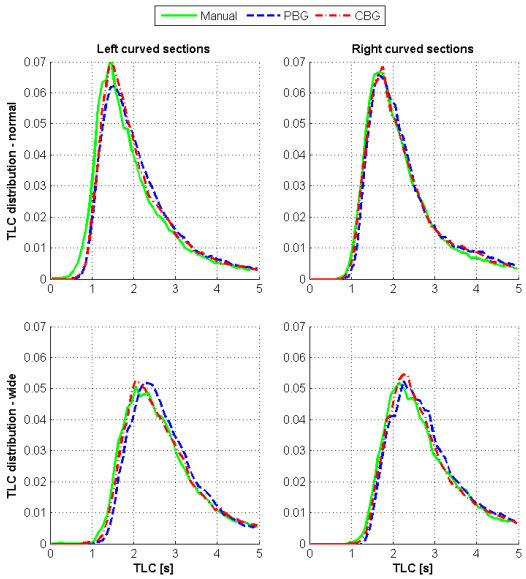

Fig. 23: Distribution of TLC, averaged over all participants, for road width 3 m (top figures) and road width 5 m (bottom figures), on left curved sections (left figures) and right curved sections (right figures). Depicted are manual driving (green, solid), driving with Performance-Based Guidance (blue, dashed), and driving with Criticality-Based Guidance (red, dash-dot). Bin size was 0.1 s.

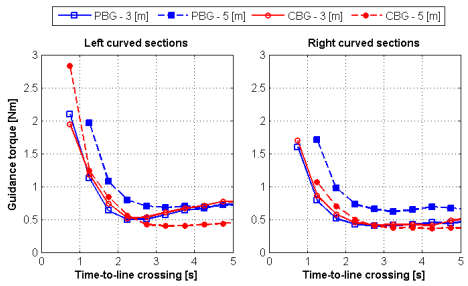

Fig. 24: Guidance torques, as a function of time-to-line crossing, for performance-based guidance (PBG, blue) and criticality-based guidance (CBG, red) on both normal road width (3 m, solid) and wide road width (5 m, dashed). TLC was binned in sections of 0.5 s and plotted against corresponding average guidance torque. The left figure depicts response in left curved sections, the right figure depicts response in right curved sections. Not all participants recorded equally low TLC values; data points can be the average of less than 24 participants. If no values were recorded for a bin, it was left empty.

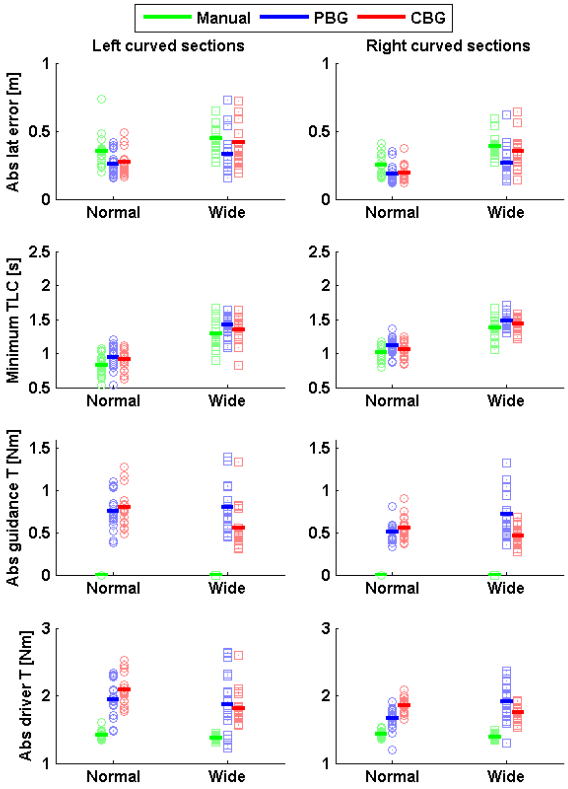

Fig. 25: Individual result and average result for all participants for mean absolute lateral error, minimum TLC, mean absolute feedback torque and mean absolute driver torque. Left column corresponds to metric on left curved sections; right column corresponds to right curved sections. Circles and squares denote individual response on normal road width (3 m) and wide road width (5 m), respectively; single values were collected by averaging response for a single condition (6 and 12 repetitions for straight and curved road sections, respectively). Horizontal bars correspond to the average over all participants, for manual driving (green), PBG (blue) and CBG (red).

APPENDIX E
QUESTIONNAIRES

Van Der Laan Questionnaire

To be filled in by investigator:

Participant nr:	Haptic Controller	Date:

My judgments of the current system are ... (please tick a box on every line)

1.	Useful	|__|__|__|__|__|	Useless
2.	Pleasant	|__|__|__|__|__|	Unpleasent
3.	Bad	|__|__|__|__|__|	Good
4.	Nice	|__|__|__|__|__|	Annoying
5.	Effective	|__|__|__|__|__|	Superfluous
6.	Irritating	|__|__|__|__|__|	Likeable
7.	Assisting	|__|__|__|__|__|	Worthless
8.	Undesirable	|__|__|__|__|__|	Desirable
9.	Raising Alertness	|__|__|__|__|__|	Sleep-inducing

Comments on the experiment and system tested: (please provide any additional comments you may have)

- -
- -
- -
- -
- -
- -
- -

NASA Task Load Index

Hart and Staveland's NASA Task Load Index (TLX) method assesses work load on five 7-point scales. Increments of high, medium and low estimates for each point result in 21 gradations on the scales.

Name	Task	Date

Mental Demand — How mentally demanding was the task?

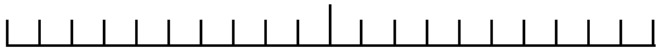

Very Low — Very High

Physical Demand — How physically demanding was the task?

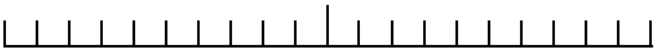

Very Low — Very High

Temporal Demand — How hurried or rushed was the pace of the task?

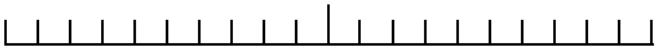

Very Low — Very High

Performance — How successful were you in accomplishing what you were asked to do?

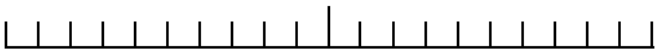

Perfect — Failure

Effort — How hard did you have to work to accomplish your level of performance?

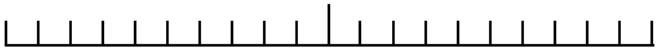

Very Low — Very High

Frustration — How insecure, discouraged, irritated, stressed, and annoyed wereyou?

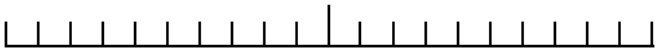

Very Low — Very High

Nausea: to what extend do you experience nausea? Please circle the statement that is most fitting to your condition:

1. Not experiencing any nausea, no sign of symptoms.
2. Arising symptoms (like a feeling in the abdomen), but no nausea.
3. Slightly nauseous.
4. Nauseous.
5. Very nauseous, retching.
6. Throwing up.